LEC Journal 2022, 4 (1): 1-6
ISSN: 2565-5205 (print)

© LEC, Pokhara University
Research Article

FESTIVAL INDUCED AIR QUALITY PERTURBATION OVER AN URBAN CENTER IN EASTERN NEPAL

[1]Sishir Dahal, [2]Binod K Bhattarai, [3]Dipesh Rupakheti, [4]Jayandra K Shrestha, [5]Ram K Sharma*

[1]Department of Civil Engineering IOE, Pulchowk Campus, TU, Lalitpur, Nepal
[2]Department of Applied Sciences and Chemical Engineering IOE, Pulchowk Campus, TU, Lalitpur, Nepal
[3]Jiangsu Key Laboratory of Atmospheric Environment Monitoring and Pollution Control, Collaborative Innovation Center of Atmospheric Environment and Equipment, School of Environmental Science and Engineering, Nanjing University of Information Science and Technology, Nanjing, China
[4]Department of Applied Sciences and Chemical Engineering IOE, Pulchowk Campus, TU, Lalitpur, Nepal
[5]Department of Applied Sciences &Chemical Engineering, IOE, Pulchowk Campus, TU, Lalitpur, Nepal
Corresponding author email*: rksharma2002@ioe.edu.np

ABSTRACT

An attempt has been made to investigate the changes in the characteristics of aerosol optical properties and a columnar load of carbon monoxide (CO) induced during the Dashain celebration 2018 over Birtamode, Nepal. Ground-based measurements of Aerosol Optical Depth (AOD) were carried out using a Microtops II sun-photometer during 13th to 25th Oct, 2018. AOD values on days before Dashain were in the range of 0.6 which increased above 1 attaining a maximum value of 1.6 on 19th. The AOD values started dropping below 1 on 24th, attaining a daily average of 0.64. The peak values on the respective days were also captured by Moderate Resolution Imaging Spectroradiometer (MODIS) AOD retrievals. A similar pattern was observed with the TROPOspheric Measuring Instrument (TROPOMI) CO column with peak value on the 19th. The air mass trajectories show that the increase in the AOD and CO values is of local origin and the CAMS GFAS wildfire flux of CO and PM2.5 show no change during the study period. However, the spatial analysis of AOD shows that the increased values are of regional nature. The results highlight the necessity of installation of low-cost air quality sensors in the region and utilization of aerosol and trace gaseous products derived from satellite remote sensing instruments at high temporal resolution and the application of chemical transport models.

Keywords—*aerosol optical depth, sun-photometer, MODIS, TROPOMI, pollution*

I. INTRODUCTION

Aerosols are suspended solid particulate materials and liquid droplets in the atmosphere having both natural and anthropogenic origin and, size ranging between 0.001 µm to 100 µm. They interact with incoming solar radiation and outgoing terrestrial long wave radiation by scattering and absorbing and produce radiative effect of cooling or warming the atmosphere. Many researcher groups around the world have confirmed the climatic impact of aerosols. Aerosols play major role deteriorating air quality and possess harmful effect in human health [1]. Certain nature of aerosols causes negative radiative forcing indirectly through formation of clouds and thereby influence cloud properties and their lifetime [2]. Similarly, some aerosols such as black carbon and mineral dust cause positive radiative forcing (warming) by absorbing solar radiation [3][4]. The direct and indirect effects of atmospheric aerosols on radiative forcing and cloud microphysics are strongly dependent on their microphysical and chemical properties [5]. Atmospheric aerosols exhibit very large spatial as well as temporal variability. Even though the natural aerosols play a very significant role on a global scale, aerosols of anthropogenic origin are very important on a regional scale [6][7]. This study is the first of its kind in the eastern Nepal and the objective of this paper is to identify the variation in the columnar load of pollutants mainly Aerosol Optical Depth (AOD) and carbon monoxide (CO) during the festive season. It also aims to validate AOD obtained from MODIS onboard Terra and Aqua satellites and to identify the long-term trend.

II. METHODS

A. Study Area

Birtamode (Fig.1) is one of the rapidly growing cities of eastern Nepal and socio-economic hub of one of the five most populated districts of the country. Based on physiographical and climatic conditions, the region can be classified as a sub- tropical with annual precipitation over 2000 mm per year. The major sources of air pollution in Birtamode include industries (mainly brick kilns), biomass burning and vehicular emissions. With an aim to understand the influence of festival on local air quality, we set up a base station in Birtamode region (26.65°N, 88°E, 137 m a.s.l) to conduct ground-based monitoring of AOD. This study was conducted during Dashain which is the biggest festival celebrated in the country. The festival is celebrated for five days during which majority of people return to their hometown to celebrate the festival with their relatives. During 2018, this festival was celebrated from 16th – 20th October. Thus we conducted the

monitoring of AOD from 13th to 25th October.

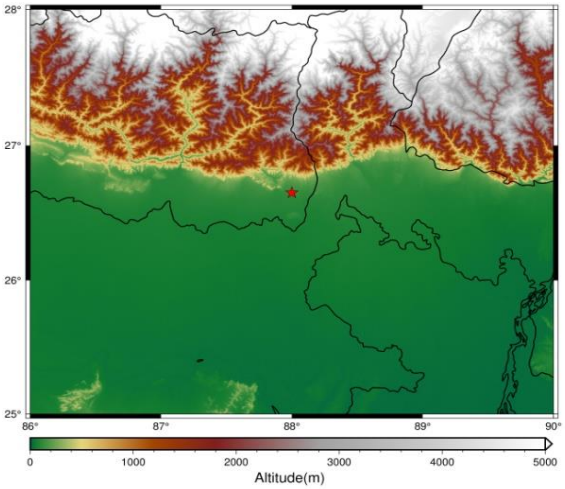

Fig. 1. Location map of study area (red star represents Birtamode)

B. Instrumentation

The ground- based spectral AOD measurements were carried out continuously from 13th to 25th October 2018 at an interval of 30 minutes from 6:30 AM to 4:30 PM local time (which is 05 hours 45 minutes ahead of GMT). We used a hand-held Microtops II sunphotometer (manufactured by Solar Light Company Inc., USA) containing five different interference filters at 340-, 440-, 500-, 675-, and 870 nm wavelengths and provides columnar information about aerosols. The sunphotometer works on the principle of extinction of solar radiation intensity at a certain wavelength and has the bandwidth of 2 nm at a 340 nm channel and 10 nm for rest of channels [8][9]. The instrument has five accurately aligned optical collimators with 2.5° as a full field of view. More details about the Microtops II characteristics, its calibration, performance and accuracy of the retrievals are provided elsewhere [10]. The spectral AOD and the Angstrom exponent (α) are two main parameters for examining the columnar aerosol loading and properties. α contains information about the size of the particle or the volume fraction of the fine versus coarse-mode particles [11] and can be determined with Angstrom's power law [12]:

$$\tau(\lambda) = \beta\lambda^{-\alpha} \quad \ldots(2)$$

$$\ln[\tau(\lambda)] = -\alpha\ln(\lambda) + \ln(\beta) \quad \ldots(3)$$

Where τ(λ) is the estimated AOD at the wavelength λ, α is the Angstrom exponent and β is the turbidity coefficient which equals to AOD at λ= 1μm. In the present study, the value of α and β are computed in the wavelength interval of 340- 870 nm, applying least square method to Eqn. 3.

C. MODIS

Moderate Resolution Imaging Spectroradiometer (MODIS) instrument makes radiance observations in 36 spectral channels at spatial resolution ranging from 250 m to 1 km with a swath width of 2300 km, allowing almost daily global coverage [13]. The MODIS sensor is onboard the polar orbiting NASA-EOS Terra and Aqua spacecrafts with equator crossing time of 10:30 and 13:30 local solar time (LST) respectively [14]. MODIS measures AOD with an estimated error of ±0.05±0.20τ [15] over the land at 0.47 and 0.66 wavelengths and extrapolates it to a 550 nm wavelength [16]. Daily AOD data (Level 2, Version C6.1) over Birtamode acquired with the MODIS instrument onboard the Terra and Aqua satellites were retrieved from the LAADS DAAC data platform of NASA (https://ladsweb.modaps.eosdis.nasa.gov/). The MODIS aerosol retrieval in this study was calculated on a 10km × 10km resolution (Level 2), which was retrieved from the higher resolution radiance measurements (Level 1B). The AOD is retrieved over the ground station within a sampling window with 3×3 pixelscentered over the ground station [17]. The data thus obtained was compared with the ground- based data obtained from sun-photometer. To maintain the consistency in data characteristics , Microtops AOD at 550nm was derived using Angstrom's power law (Eqn. 2) where α and β were estimated from Microtops derived AODs in the spectra ranging from 340 to 870 nm.

D. TROPOMI

TROPOspheric Monitoring Instrument (TROPOMI) is a sensor onboard Sentinel-5 Precursor (S5P) satellite launched on 19 October 2017 by the European Space Agency which is focused on air quality and composition-climate interaction. TROPOMI observes the CO global abundance exploiting clear-sky and cloudy-sky Earth radiance measurements in the 2.3μm spectral range of the shortwave infrared (SWIR) part of the solar spectrum. The S5P orbit is a sun-synchronous orbit with an ascending node equatorial crossing at 13:30 mean local solar time. The orbit reference altitude is approximately 824km with an inclination of 98.7° [18]. The wide across-track field-of-view (FoV) of 108° provides a wide swath of about 2600 km and thus almost globally allows for daily coverage of the earth. The level 2 TROPOMI CO product used in this study have been downloaded from the GES DISC data platform (https://disc.gsfc.nasa.gov/). For the study duration, the data is available at the resolution of 7km×7km. We ignore the vertically integrated CO column with qa_value lesser than 0.5. The first validation study showed that the TROPOMI data are in good agreement with the Copernicus Atmosphere Monitoring Service (CAMS) data. For the India region, a 2.9% difference was found with a standard deviation of 6% and a Pearson correlation of 0.9 [19].

E. HYSPLIT

The National Oceanic and Atmospheric Administration (NOAA) Air Resource Laboratory's (ARL) Hybrid Single-Particle Lagrangian Integrated Trajectory (HYSPLIT) model is a complete system for computing simple air parcel trajectories as well as complex transport, dispersion, chemical transformation, and deposition simulations. One of the most common model applications is a back- trajectory analysis to determine the origin of air masses and have been used for plethora of applications throughout the world [20]. Due to the increase requirement of access to tools to analyze and predict the transport and dispersion of pollutants in the atmosphere, a unique web- based Real- time Environmental Applications and Display sYstem (READY) has been under continuous development since 1997. READY provides a "quasi- operational" portal to run the HYSPLIT atmospheric transport and dispersion model and interpret its result [21].

F. Error Analysis

The Microtops II sun-photometer was used for the first time in eastern Nepal (Birtamode), so, special care was taken while making observations and also in the retrievals of spectral AODs and computation of Angstrom's parameters. To avoid any possible cloud contamination, measurements were only done on clear days, with few or no clouds covering the sky or clouds far from, the sun disk. From the scans the higher values suspected to have been affected from undetected thin cirrus clouds have been removed. From the new dataset, the spectrums that calculated AODs beyond the daily mean ± 2σ were also excluded from the analysis. During this stage the majority of the cases that were excluded correspond to high AODs (especially at longer wavelengths) and to very low α values suggesting cloud contamination [22].

Since spectral AOD presents a curvature in log-log coordinates due to inaccuracies in the fit of the Angstrom's formula [23] the consistency in the retrievals of Angstrom exponent via different methods give credit to the accuracy of the spectral AOD retrievals and minimizes the curvature effect [24]. So, α values obtained from the linear fit method (LFM, total use of five wavelengths) with those obtained from the Volz method (VM, use of two wavelengths) have been correlated (Fig. 2). The results show an excellent correlation (R^2= 0.995) between LFM and VM. The slope value close to 1 and negligible intercept indicate great accuracy in the retrievals of α and, therefore to the spectral AOD [22].

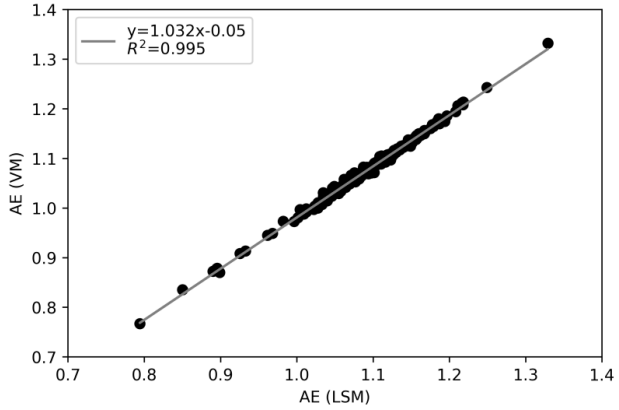

Fig. 2. Correlation between AE values obtained from Volz method (VM) and linear fit method (LFM)

III. RESULTS AND DISCUSSIONS

A. Spectral Dependence of AOD

To examine the influence of Dashain festival on spectral variations of AOD for forenoon (8:00 LST), noon and afternoon (16:00 LST) during pre-Dashain days (average of three days before Dashain, 13th to 15th October), Dashain days (average of five days, 16th to 20th October) and five consecutive days after Dashain are evaluated. It is observed that there is significant increase in AOD during Dashain festival in all wavelengths. AOD500 (AOD at 500nm wavelength) increased from 0.41 to 1.36, 0.51 to 1.38 and 0.60 to 1.52 respectively at forenoon, noon, and afternoon. From 21st, AOD values start decreasing suggesting settling of aerosols and reduced production.

To understand the influence of Dashain festival on wavelength dependence of AOD, hour to hour spectral variations of AOD for pre-Dashain days, during Dashain and following days of Dashain are shown in Fig. 3. The conspicuous feature of this data is a significant increase in AOD during Dashain compared to pre-Dashain days, especially for shorter wavelength. However, the value seems to decrease for the post-Dashain days. The difference between AOD at 340nm and AOD at 870nm in morning and evening hours for pre-Dashain days were 0.37 and 0.64 respectively. But the difference has changed significantly during Dashain days with 1.13 and 1.23 in morning and evening respectively. This suggests a change in the size distribution pattern of aerosols in the atmosphere with an increase in smaller sized aerosols that may be attributed to the residential burning during festival.

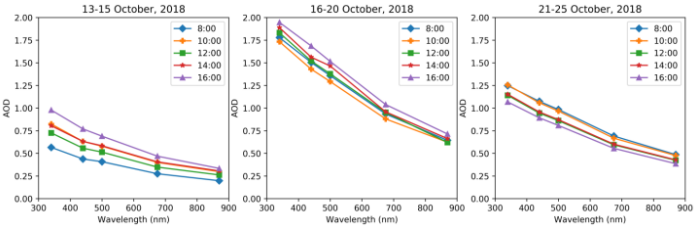

Fig. 3.Spectral variation of AOD (a) before, (b) during and (c) after Dashain festival

B. Variation of Daily Mean AOD and Angstrom's Parameter

The average value of AOD for individual days from 13th to 25th October, 2018 for all five wavelengths is plotted in Figure 4. It shows a notable increase in AOD from 16th to 19th October with the highest value on 19th October. The value gradually dropped to pre-Dashain condition on 24th October. On 16th, AOD increased by 151.94%, 159.13%, 149.02%, 149.82%, and 139.9% respectively for 340nm, 440nm, 500nm, 675nm, and 870nm. The percentage increment at lower wavelengths being the highest explains the dominance of fine mode particles.

The daily variation in Angstrom exponent (α) and turbidity parameter (β) calculated based on daily average AOD values for the period 13th to 25thOctober are also shown in Fig. 4. Angstrom exponent changed only slightly, but turbidity parameter showed a prominent rise from around 0.248 on day before Dashain to 0.615 during Dashain. On pre-Dashain days, α and β show a negative correlation as expected, but during Dashain sudden increment of AOD from 15th to 16th and gradual decrement of AOD from 19th to 20th Ocotber, negative correlation is not observed.

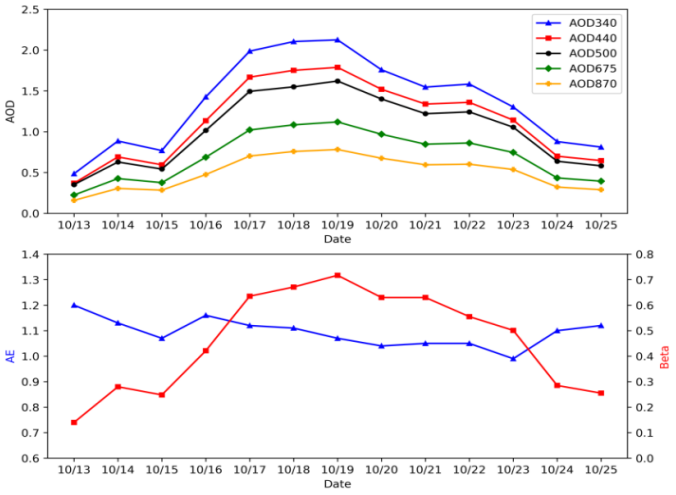

Fig. 4. Daily variation of (a) AOD and (b) AE and β

C. Variation of MODIS AOD

The MODIS AOD data obtained from Terra and Aqua satellite was compared with the Microtops data at ±30 minutes of the respective satellite overpass. The MODIS AOD values show excellent correlation with the ground based observations made by Microtops. Fig. 5 shows the scatter plots between two parameters (satellite- based and ground-based AOD) for the study period. The R^2 values for Microtops AOD versus MODIS AOD are 0.8486 and 0.8777 respectively for Aqua and Terra respectively. These values are much higher compared to that obtained at Lumbini i.e., 0.62 and 0.66 for Terra and Aqua respectively [25]. The higher R^2 value for Birtamode is attributed to comparison of instantaneous AODs at ±30 minutes of Terra and Aqua overpass compared to the daily averaged AODs taken in Lumbini.

The variation of MODIS AOD along with the Microtops AOD at the nearest time of satellite overpass is shown in Fig. 6. It shows that MODIS captures the peak values of AOD as seen from the ground based measurements and demonstrates the similar trend during the study period. To verify the peak values obtained during Dashain, 5-year (2013-2017) averaged AOD values retrieved from MODIS have been plotted (not shown here). The analysis shows that the AOD values peak around day 5, 6, and 7, which is quite similar to that obtained from ground based measurements in 2018, and illustrates that the higher values of AOD in Birtamode and the surrounding during Dashain is a usual phenomenon.

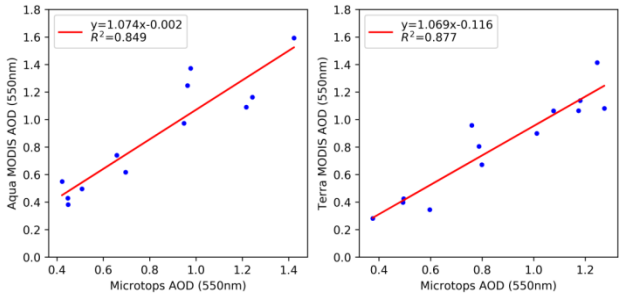

Fig. 5. Scatter plot showing Microtops AOD and MODIS AOD

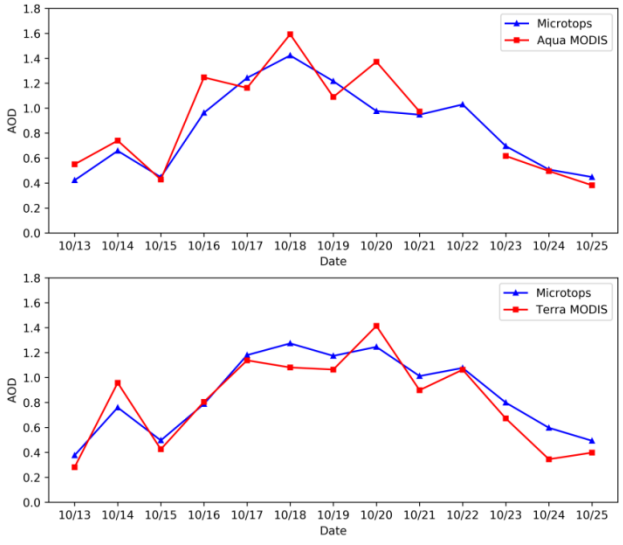

Fig.6. Variations of Microtops AOD and MODIS AOD

D. Classifications of Aerosols

In order to identify the changes in the aerosol types, aerosol classification is done by correlating AOD and α [26]. The scatter plot (Fig. 7) between AOD and α is used to classify different aerosol types over Birtamode. Based on literature, five dominant aerosol types are identified, viz., clean background condition (CBC), mostly dust (MD), anthropogenic aerosol (AA; mainly coming from urban/industrial regions around the measuring site and, as well as from vehicular emissions), biomass burning (BB), and mixed type (MT) aerosol. We have used the similar threshold over Varanasi in India [27] as: AOD<0.3 and α<0.9 (CBC); AOD>0.7 and α<0.6 (MD); 0.3≤AOD≤1 and α>0.9 (AA); AOD>1.0 and α>1.0 (BB). The cases that don't belong to above mentioned categories are inferred as MT aerosols.

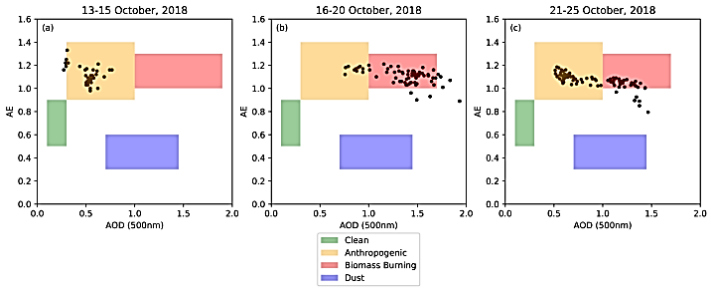

Fig. 7. Scatter plot between AOD and AE

From the figure, it is clear that the AA type has maximum contribution (~86.5%) before Dashain which is replaced by BB (~82%) during Dashain. The drastic change in the aerosol contribution by BB is mainly attributed to the celebration induced emission which basically includes the emission from burning fire woods and other biomass. The BB aerosol type is more frequent during post- monsoon due to extensive agro-residue burning in the IGP [25].

E. Variation in columnar CO

The variation of TROPOMI CO column during the study period is shown in Fig. 8. The trend of CO column is similar to that of AOD with the highest value 0.0482 mol/m^2 on 19th October. The CO value gradually decreases from 20th October attaining nearly pre-Dashain level on 25th October. Most of the earlier studies in the IGP region explain that the higher level of air pollutants during post-monsoon (Oct-Nov) is mainly due to the emission form the excessive agro-mass burning in the north-western part of the IGP which is carried by the air masses to other region [28][29][30][25].

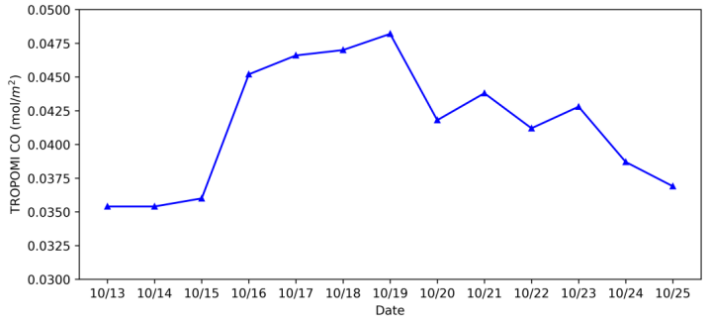

Fig. 8. Variation of TROPOMI columnar CO

However, the latest study conducted by [31] reveals that the residential and commercial burnings are the major contributor to

increased CO during the high pollution episodes in the post-monsoon season. Thus, increment in columnar CO over the study site during Dashain festival may indicate the enhanced contribution of residential burning during the festival.

F. Transboundary effect on air quality

In order to understand the possible origin regions and transport pathways of air masses and thus the air pollutants, back trajectory analysis has been carried out as done in previous studies [25][32][33]. One- day air- mass back trajectories are plotted for the 15th, 16th, 19th and 25th October at the height of 500m and 1000m using HYSPLIT model from the Air Resource Laboratory of NOAA (not shown here). The trajectories for 15th and 16th October are quite similar as the air masses pass over the same region before reaching Birtamode. However, the AOD and CO values on 16th October are much higher compared to 15th October. Similarly, the AOD and CO values on 25th October are lower compared to 19th October even when the trajectories look almost similar. Moreover, the MODIS fire product demonstrates that there is no significant change in the fire around the study region during the study period (not shown here). Besides, the graph clearly shows that the north-west region of IGP has higher fire counts compared to other region. However, the CAMS Global Fire Assimilation System shows that the wildfire flux of CO and PM2.5 in Birtamode during the study duration is nil (not shown here). This further explains that the higher values of AOD and CO are due to local activities which are due to local activities that are not associated with residual agro-mass burning (open fires).

IV. CONCLUSIONS

The ground- based observations of Microtops II sun-photometer were analyzed at an urban station in eastern Nepal (Birtamode), during Dashian festival and compared with satellite retrievals. The results of the analysis suggest that the higher value of AOD observed during Dashain festival has been justified by the MODIS AOD values. TROPOMI CO column showed the trend similar to AOD values. The MODIS AODvalues showed good correlation with ground-based sun-photometer. Moreover, MODIS AOD variation showed similar trend during Dashain festival based on 2018 data and 5- year (2013- 2017) averaged data. The HYSPLIT back trajectories along with the MODIS fire plot and CAMS GFAS wildfire flux of CO and PM2.5 explains that the peak values of AOD and CO during Dashain was of local origin. Moreover, the results suggest the possible utilization of MODIS data sets in understanding the long term trend of aerosol characteristics in Birtamode. It also opens the gateway for further detailed studies to identify the local source of pollutants during Dashain festival. However, the spatial analysis of MODIS AOD (Fig. 9) reveals that the increased value of AOD was a regional phenomenon during Dashain 2018 thus highlighting the haze episode in the Indo- Gangetic Plain (IGP), which requires further detailed study. The high value of AOD along the IGP, including the current study area underscores the need of installation of low cost air quality sensors at different locations and application of aerosol and other gaseous products based on satellite remote sensing data of high temporal resolution.

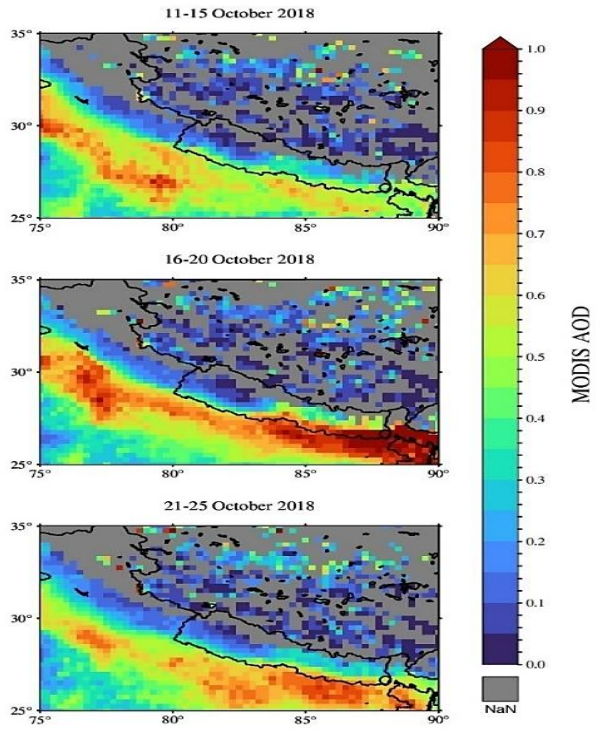

Fig. 9. Spatial distribution of MODIS AOD (black circle represents Birtamode region)

ACKNOWLEDGMENT

Sishir Dahal acknowledges the Department of Applied Sciences and Chemical Engineering, Pulchowk Campus, IOE, Tribhuvan University for providing Microtops II sunphotometer used for this study. MODIS data have been obtained from NASA LAADS DAAC data archive and the authors would like to thank MODIS team for developing the AOD product.

REFERENCES

[1] Stocker, T.F., Qin, D., Plattner, G.K., Tignor, M.M., Allen, S.K., Boschung, J., Nauels, A., Xia, Y., Bex, V. and Midgley, P.M., 2014. Climate Change 2013: The physical science basis. contribution of working group I to the fifth assessment report of IPCC the intergovernmental panel on climate change.

[2] Penner, J.E., Zhang, S.Y. and Chuang, C.C., 2003. Soot and smoke aerosol may not warm climate. *Journal of Geophysical Research: Atmospheres*, *108*(D21).

[3] Kaufman, Y.J., Tanré, D. and Boucher, O., 2002. A satellite view of aerosols in the climate system. *Nature*, *419*(6903), pp.215-223.

[4] Lohmann, U. and Feichter, J., 2005. Global indirect aerosol effects: a review. *Atmospheric Chemistry and Physics*, *5*(3), pp.715-737.

[5] Hegg, D.A., Hobbs, P.V., Gassó, S., Nance, J.D. and Rangno, A.L., 1996. Aerosol measurements in the Arctic relevant to direct and indirect radiative forcing. *Journal of Geophysical Research: Atmospheres*, *101*(D18), pp.23349-23363.

[6] Kaufman, Y.J. and Fraser, R.S., 1983. Light extinction by aerosols during summer air pollution. *Journal of Applied Meteorology and Climatology*, *22*(10), pp.1694-1706.

[7] Ramachandran, S., Srivastava, R., Kedia, S. and Rajesh, T.A., 2012. Contribution of natural and anthropogenic aerosols to

optical properties and radiative effects over an urban location. *Environmental Research Letters*, *7*(3), p.034028.

[8] Sharma, N.P., 2017. Variations of aerosol optical depth in bhaktapur, nepal. *Journal of the Institute of Engineering*, *13*(1), pp.133-138.

[9] Tiwari, S., Kaskaoutis, D., Soni, V.K., Attri, S.D. and Singh, A.K., 2018. Aerosol columnar characteristics and their heterogeneous nature over Varanasi, in the central Ganges valley. *Environmental Science and Pollution Research*, *25*(25), pp.24726-24745.

[10] Morys, M., Mims III, F.M., Hagerup, S., Anderson, S.E., Baker, A., Kia, J. and Walkup, T., 2001. Design, calibration, and performance of MICROTOPS II handheld ozone monitor and Sun photometer. *Journal of Geophysical Research: Atmospheres*, *106*(D13), pp.14573-14582.

[11] Schuster, G.L., Dubovik, O. and Holben, B.N., 2006. Angstrom exponent and bimodal aerosol size distributions. *Journal of Geophysical Research: Atmospheres*, *111*(D7).

[12] Ångström, A., 1964. The parameters of atmospheric turbidity. *Tellus*, *16*(1), pp.64-75.

[13] Gupta, P., Khan, M.N., da Silva, A. and Patadia, F., 2013. MODIS aerosol optical depth observations over urban areas in Pakistan: quantity and quality of the data for air quality monitoring. *Atmospheric pollution research*, *4*(1), pp.43-52.

[14] Levy, R.C., Remer, L.A., Mattoo, S., Vermote, E.F. and Kaufman, Y.J., 2007. Second-generation operational algorithm: Retrieval of aerosol properties over land from inversion of Moderate Resolution Imaging Spectroradiometer spectral reflectance. *Journal of Geophysical Research: Atmospheres*, *112*(D13).

[15] Chu, D.A., Kaufman, Y.J., Ichoku, C., Remer, L.A., Tanré, D. and Holben, B.N., 2002. Validation of MODIS aerosol optical depth retrieval over land. *Geophysical research letters*, *29*(12), pp.MOD2-1.

[16] Hsu, N.C., Jeong, M.J., Bettenhausen, C., Sayer, A.M., Hansell, R., Seftor, C.S., Huang, J. and Tsay, S.C., 2013. Enhanced Deep Blue aerosol retrieval algorithm: The second generation. *Journal of Geophysical Research: Atmospheres*, *118*(16), pp.9296-9315.

[17] Mhawish, A., Banerjee, T., Broday, D.M., Misra, A. and Tripathi, S.N., 2017. Evaluation of MODIS Collection 6 aerosol retrieval algorithms over Indo-Gangetic Plain: Implications of aerosols types and mass loading. *Remote sensing of environment*, *201*, pp.297-313.

[18] Landgraf, J., Scheepmaker, R., Borsdorff, T., Hu, H., Houweling, S., Butz, A., Aben, I. and Hasekamp, O., 2016. Carbon monoxide total column retrievals from TROPOMI shortwave infrared measurements. *Atmospheric Measurement Techniques*, *9*(10), pp.4955-4975.

[19] Borsdorff, T., Aan de Brugh, J., Hu, H., Aben, I., Hasekamp, O. and Landgraf, J., 2018. Measuring carbon monoxide with TROPOMI: First results and a comparison with ECMWF-IFS analysis data. *Geophysical Research Letters*, *45*(6), pp.2826-2832.

[20] Stein, A.F., Draxler, R.R., Rolph, G.D., Stunder, B.J., Cohen, M.D. and Ngan, F., 2015. NOAA's HYSPLIT atmospheric transport and dispersion modeling system. *Bulletin of the American Meteorological Society*, *96*(12), pp.2059-2077.

[21] Rolph, G., Stein, A. and Stunder, B., 2017. Real-time environmental applications and display system: READY. *Environmental Modelling & Software*, *95*, pp.210-228.

[22] Sharma, M., Kaskaoutis, D.G., Singh, R.P. and Singh, S., 2014. Seasonal variability of atmospheric aerosol parameters over Greater Noida using ground sunphotometer observations. *Aerosol and air quality research*, *14*(3), pp.608-622.

[23] Kaskaoutis, D.G. and Kambezidis, H.D., 2006. Investigation into the wavelength dependence of the aerosol optical depth in the Athens area. *Quarterly Journal of the Royal Meteorological Society: A journal of the atmospheric sciences, applied meteorology and physical oceanography*, *132*(620), pp.2217-2234.

[24] Kaskaoutis, D.G. and Kambezidis, H.D., 2008. Comparison of the Ångström parameters retrieval in different spectral ranges with the use of different techniques. *Meteorology and Atmospheric Physics*, *99*(3), pp.233-246.

[25] Rupakheti, D., Kang, S., Rupakheti, M., Cong, Z., Tripathee, L., Panday, A.K. and Holben, B.N., 2018. Observation of optical properties and sources of aerosols at Buddha's birthplace, Lumbini, Nepal: environmental implications. *Environmental Science and Pollution Research*, *25*(15), pp.14868-14881.

[26] Kaskaoutis, D.G., Badarinath, K.V.S., Kumar Kharol, S., Rani Sharma, A. and Kambezidis, H.D., 2009. Variations in the aerosol optical properties and types over the tropical urban site of Hyderabad, India. *Journal of Geophysical Research: Atmospheres*, *114*(D22).

[27] Tiwari, S., Kaskaoutis, D., Soni, V.K., Attri, S.D. and Singh, A.K., 2018. Aerosol columnar characteristics and their heterogeneous nature over Varanasi, in the central Ganges valley. *Environmental Science and Pollution Research*, *25*(25), pp.24726-24745.

[28] Gani, S., Bhandari, S., Seraj, S., Wang, D.S., Patel, K., Soni, P., Arub, Z., Habib, G., Hildebrandt Ruiz, L. and Apte, J.S., 2019. Submicron aerosol composition in the world's most polluted megacity: the Delhi Aerosol Supersite study. *Atmospheric Chemistry and Physics*, *19*(10), pp.6843-6859.

[29] Tiwari, S., Pandithurai, G., Attri, S.D., Srivastava, A.K., Soni, V.K., Bisht, D.S., Kumar, V.A. and Srivastava, M.K., 2015. Aerosol optical properties and their relationship with meteorological parameters during wintertime in Delhi, India. *Atmospheric Research*, *153*, pp.465-479.

[30] Tiwari, S., Bisht, D.S., Srivastava, A.K., Pipal, A.S., Taneja, A., Srivastava, M.K. and Attri, S.D., 2014. Variability in atmospheric particulates and meteorological effects on their mass concentrations over Delhi, India. *Atmospheric research*, *145*, pp.45-56.

[31] Dekker, I.N., Houweling, S., Pandey, S., Krol, M., Röckmann, T., Borsdorff, T., Landgraf, J. and Aben, I., 2019. What caused the extreme CO concentrations during the 2017 high-pollution episode in India?. *Atmospheric Chemistry and Physics*, *19*(6), pp.3433-3445.

[32] Tripathee, L., Kang, S., Rupakheti, D., Zhang, Q., Huang, J. and Sillanpää, M., 2016. Water-soluble ionic composition of aerosols at urban location in the foothills of Himalaya, Pokhara Valley, Nepal. *Atmosphere*, *7*(8), p.102.

[33] Kaskaoutis, D.G., Gautam, R., Singh, R.P., Houssos, E.E., Goto, D., Singh, S., Bartzokas, A., Kosmopoulos, P.G., Sharma, M., Hsu, N.C. and Holben, B.N., 2012. Influence of anomalous dry conditions on aerosols over India: transport, distribution and properties. *Journal of Geophysical Research: Atmospheres*, *117*(D9).